Determination of proper frequency range for accurate heat capacity measurement by AC microcalorimeter

Olivier Riou, Jean Félix Durastanti, Youssef Sfaxi

reprint: Superlattices and Microstructures **35** (2004), pp. 353-361

Determination of proper frequency range for accurate heat capacity measurement by AC micro calorimetry

Olivier Riou[1], Jean-Felix Durastanti[2], Youssef Sfaxi[2]

1. Laboratoire Universitaire des Sciences Appliquées de Cherbourg – LUSAC, Iut Cherbourg Manche, Université de Caen Basse Normandie, 50130 Cherbourg-en-Cotentin, France
2. Centre de recherche en thermique et environnement des systèmes – CERTES, IUT de Sénart-Fontainebleau, Université Paris XII, Avenue Pierre Point, 77127 Lieusaint, France

Corresponding author: **olivier.riou@u-pec.fr**
Version: **Wednesday, August 16, 2023**

Abstract. We study the frequency response of a micro calorimeter implementing an oscillating temperature regime. The micro calorimeter combines a free-standing membrane together with lithographic techniques that allow to fit the sample-holder to be adapted to samples of a few micrograms. We show that the conventional model of Sullivan and Seidel is inaccurate due to of the contributions of the addenda contributions. We propose an error function that takes into account the influence parameters of the four body sample-holder (sample, membrane, sensors and gold isotherm). By minimizing the error function, we propose conditions to adjust the frequency domain measurement in order to improve the accuracy of the heat capacity measurements.

Note to the lectors

This version is a pre-publication of the article published in the journal of Superlattices and Microstructures (2004). The present document required a careful re-reading of the document. Errors were identified and corrected by myself, while maintaining the structure of the document, which was proofread by my expert colleagues. I also improved graphic charts to give the reader a better reading of the work.

Please do not hesitate to send me your comments or questions to olivier.riou@u-pec.fr. I will give you answer and it will help me to improve the quality of this publication.

Olivier **Riou**

https://doi.org/10.1016/j.spmi.2003.11.006

Nomenclature

t	Thickness, m	A	Surface, m²
κ	Thermal conductivity, $W\,K^{-1}\,m^{-1}$	ρ	Specific mass, $kg\,m^{-3}$
c	Specific heat capacity, $J\,kg^{-1}\,K^{-1}$	ω	Pulsation of the thermal excitation, rad/s
τ	Periodicity of the temperature oscillation, s	k	Surface thermal conductivity, $Wm^{-2}K^{-1}$
D_x	Direcional thermal diffusivity, $D_x = \kappa/\rho c$, m^2s^{-1}	L_x	Directional thermal prenetration length, $L_x = \sqrt{2D/\omega}$, m
α	Proportion of RMS probed length, dimensionless	x	RMS length of thermal penetration, $x = \alpha \times L_x$, m
k_x	Directional wave vector of the heat propagation, m^{-1}	X	Variable of the heat propagation, $X = k_x\,x$, dimensionless
TF	Transfer function, dimensionless	$erf(\omega)$	Error function, dimensionless
K	Thermal conductance, W/K	C	Heat capacity, J/K
τ_1	Adiabatic time constant, s	τ_2	Quasistatic time constant, s
τ_e	Exchange time constant C/K, s	τ_i	Internal time constant $\tau_i = t^2/(\sqrt{90} \times D)$, s
m	Filling factor C_s/C_t, dimensionless	T_{static}	Amplitude of the static temperature of the cell, K
$\tilde{T}_s$	Peak amplitude of the oscillating sample temperature, K	$\tilde{T}$	Peak amplitude of the oscillating sample-holder temperature, K
$\dot{Q}(t)$	Thermal power excitation, W	P_θ	Joule effect peak amplitude of the dc power dissipated inside the thermometer, W
C	Contribution of the sample-holder to the heat capacity, J/K	$C_\omega(\omega)$	Diffusive contribution of the wires to the heat capacity, $C_\omega(\omega) = C_\omega \times \omega^{-0.5}$, J/K

https://doi.org/10.1016/j.spmi.2003.11.006

1. Introduction

For thirty-five years, AC modulation calorimetry has been known as the most sensitive technique for measuring thermophysical properties of a small sized sample. A review of its main applications is given in [1]. It has been successfully applied to both solid and liquid samples. Today, it is implemented in numerous micro- and nano-scale measurements that require a high resolution: let us mention the specific heat [2], the thermoelectric power, the electrical resistance temperature derivative [3].

Initially performed at low temperature, AC modulation calorimetry is now extended to ambient temperature to measure samples with masses ranging from 10 µg to 100 mg with an absolute accuracy of 1%. The resolution achieved is 10^{-4} in specific heat and 1-10 mK in temperature. These capabilities are useful for phase transition studies of the superconducting compound $YBa_2Cu_3O_{7-\delta}$ [4].

In practice, several problems arise. The most important of them is how to achieve a homogeneous temperature in a standard cell (sample, sample holder and sensors). In this way, microlithographic techniques are useful for fabricating compact measurement systems [5]. Microlithographic techniques can greatly reduce the thermal mass by integrating sensors as well as addenda contribution, which makes the device easily fit to very small samples. Due to the high viability of the process, thermal couplings are fairly well reproducible, making the behavior of sensors predictable.

The second problem is the choice of the measurement frequency since the accuracy of the measurement depends on its choice. Only a detailed study of the dynamic behavior of the cell allows to identify the frequency measurement range. The measurement frequency is guided by the criteria of quasi-staticity and adiabaticity. In modulated calorimetry, two time constants play an critical role: the adiabatic time constant τ_c and the quasistatic time constant τ. The adiabatic time constant determines the typical time for heat exchange between the system and a thermal bath, while the quasi-static time constant determines the typical time required for the system to homogenize its internal temperature. Accurate measurements are possible when the steady-state conditions are satisfied: $\omega\tau_c \gg 1$ (adiabatic condition) and $\omega\tau \ll 1$ (quasi-static condition). These conditions are found by the analyzing the $T_{ac} \times \omega$ versus ω characteristic (T_{ac} is the amplitude of temperature oscillation at the frequency f and $\omega=2\pi f$): The frequency range where $T_{ac} \times \omega = cte$ defines then the frequencies at which the steady-state conditions are met.

For sample masses of a few micrograms, the contribution of the sample holder blurs the reading of the $T_{ac} \times \omega$ curve, both because of its heat capacity contribution, which is of the same order as that of the sample, and because of the diffusive contribution to the total heat capacity due to the heat propagation along the connecting wires. On the other hand, none of the papers found in the literature describe the frequency behavior of the cell, which makes it difficult to verify unambiguously for small samples. Greene et al. [6] studied the case of a sample suspended by wire thermocouples. Such behavior was subsequently observed in references [2, 7, 8]. More recently, Minakov [9] described the effects of the sample-holder and of the heat leakage into the thermocouple wires on the measured temperature oscillation of a sandwich-type cell.

In this paper, we will propose an analytical error function within the four-body model that allows the bulk and the diffusive contributions to heat capacity measurements to be separated. We describe the typical frequency behavior of a free-standing cell. We conclude with some recommendations for improving specific heat measurements in AC modulation calorimetry.

2. State of the art

Sullivan & Seidel [10] first gave a detailed description of a measurement system using the AC technique. In their study, the thermometer and the heater are directly stuck on the sample and connected to a thermal bath via a thermal resistance K_B:

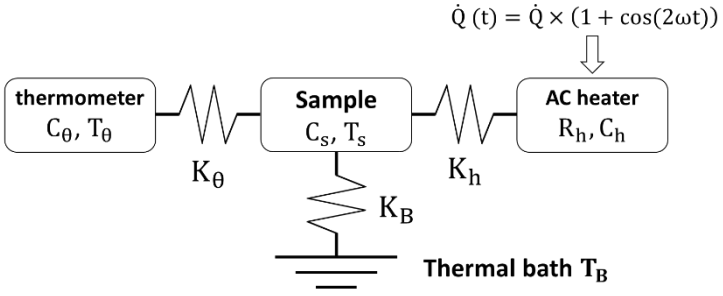

Figure 1. Three-body cell. The heat capacities of the sample, of the thermometer and of the heater are denoted by C_s, C_θ and C_h respectively, while K_θ and K_h are the thermal conductances with the sample. K_B is the thermal conductance of the cell to the thermal bath. $R_h[\Omega]$ is the electrical resistance of the AC heater.

The AC heater is generally based on the Joule effect. When an alternating current $I_h = I_{AC}\cos(\omega t)$ biases the heater, the dissipated power $\dot{Q}(t) = P_h \times (1 + \cos(2\omega t))$ imposes an oscillating temperature regime of the cell. The amplitude of the AC power is $\dot{Q} = (R_h I_{AC}^2)/2$, according to the Carnot formula. The temperature of the sample is then $T_s(t) = T_B + P_h/K_B + \dot{Q}/(\omega C_t) \times \cos(2\omega t - \varphi)$. The dephasing φ quantifies the 2ω shift time between the oscillating temperature $\widetilde{T}_s(t)$ term and the $\dot{Q}(t)$ excitation term.

In steady-state conditions, the comparison of the amplitude of the oscillating temperature $\widetilde{T}_s$ to the amplitude of AC power $\dot{Q}$ allows to quantify the total heat capacity $C_t = C_s + C_\theta + C_h$ of the cell:

$$C_t = \frac{\dot{Q}}{\omega \times \widetilde{T}_c} \qquad (1)$$

Some precautions are important to check: first, the AC power term should be low enough so that the sample is probed in an isothermal state; second, the thermal conductances have no heat capacity and third; the thermometer and the heater have an infinite thermal diffusivity so that their frequency response could be considered as instantaneous.

In Figure 1, the oscillating temperature of the cell results from the simultaneous heat exchange of three bodies (sample, thermometer and AC heater). The heat exchanges are governed by first-degree differential equations that balance the input and the output heat of each body. In a development of the 1st order in ω^2 and $1/\omega^2$, the amplitude of the oscillating cell temperature is then given by Equation 2:

$$\widetilde{T}_c(\omega) = \frac{\dot{Q}}{\omega C_t \sqrt{1 + \frac{1}{(\omega\tau_1)^2} + (\omega\tau_2)^2}} \qquad (2)$$

The adiabatic time constant of the cell is $\tau_1 = (C_s + C_\theta + C_h)/K_B$. Its quasi-static time constant is $\tau_2 = (\tau_\theta^2 + \tau_h^2)^{0.5}$ where $\tau_{e,\theta} = C_\theta/K_\theta$ and $\tau_{e,h} = C_h/K_h$ are the exchange time constants of the thermometer and of the AC heater to the sample respectively. Comparing Equation 2 with Equation 1, we highlight that the total heat capacity cannot be accurately quantified with accuracy because its value depends on the term $(1 + (1/\omega\tau_1)^2 + (\omega\tau_2)^2)^{0.5}$:

The time constants τ_1 and τ_2 then limit the accuracy of the heat capacity measurements. If the frequency is properly selected, their effects can be minimized. For example, if $10 \times \omega\tau_2 \ll 1 \ll \omega\tau_1/10$, the heat capacity quantification from Eq. 1 is performed with an accuracy of 1%. otherwise, any deviation to these conditions is quantified by the error function [11]:

$$\mathrm{erf}\,(\omega) = 1 - (1 + (1/\omega\tau_1)^2 + (\omega\tau_2)^2)^{-0.5} \qquad (3)$$

The first source of error is the thermal resistance of the sensors. Basically, the exchange times act as a low-pass frequency filter allowing heat transfer only when the measurement frequency is compatible with their exchange time values. When this condition is met, the cell oscillates in quasi-static manner. The effects on the heat capacity measurement have been studied by Velichkov [12] and Gmelin [13].

The second source of error is from the finite thermal diffusivity D of the cell components. Their values determine the amplitude of the thermal penetration length L that probe each component. L is inherently frequency and direction dependent. The directional dependence arises from the possible anisotropy of the heat transfer. For example, Sullivan & Seidel consider a transverse thermal penetration along the sample thickness t. It must be verified that $\mathrm{L}(\omega)/\mathrm{t}$ is large enough to probe the sample in its bulk, or by equivalence, its internal time constant $\tau_{\mathrm{i,s}}$ is small enough compared to the period of the temperature oscillation. This should be the same for the other components such as the sensors and the sample-holder.

The third source of error is from the diffusive leakage due to the heat propagation along the leads. The diffusive contribution increases as the sample size decreases. The frequency contribution is more difficult to formalize. The problem has been pointed out by [6].

A detailed analysis of the sources of error is necessary to identify the characteristics of the cell in order to improve the accuracy of heat capacity measurement. The analysis depends on the architecture of the cell by considering each component as an independent body with its own heat capacity and internal time constant.

An elegant way to minimize the error function is to analyze the frequency response of the cell. This involves determining the frequency range where the adiabatic and quasi-static conditions are fully satisfied.

3. Free-standing thin film membrane technology

Free-standing membrane technology offers polyvalent design solutions: it ensures a thermal management of the heat transfers and allows to the micromachining through the use of lithographic techniques for in-situ sensor deposition as well as the reduction of the addenda contributions.

The type of the membrane is versatile: the use of a silicon-based membrane has already been reported in the literature [14], and it produces very thin supports. Based on the crystalline structure of silicon, a network adaptation under layers allow optimal in-situ growth of any type of crystalline sample. The membrane is compatible with low to high temperature operating conditions, including during the sample deposition process and its subsequent heat capacity characterization.

The use of polymer-based membrane completes the technical capabilities: it produces flexible membranes that accept the bonding of bulk samples without the risk of cell rupture [2].

The thermal diagram of a typical free-standing membrane cell is presented in Figure 2.

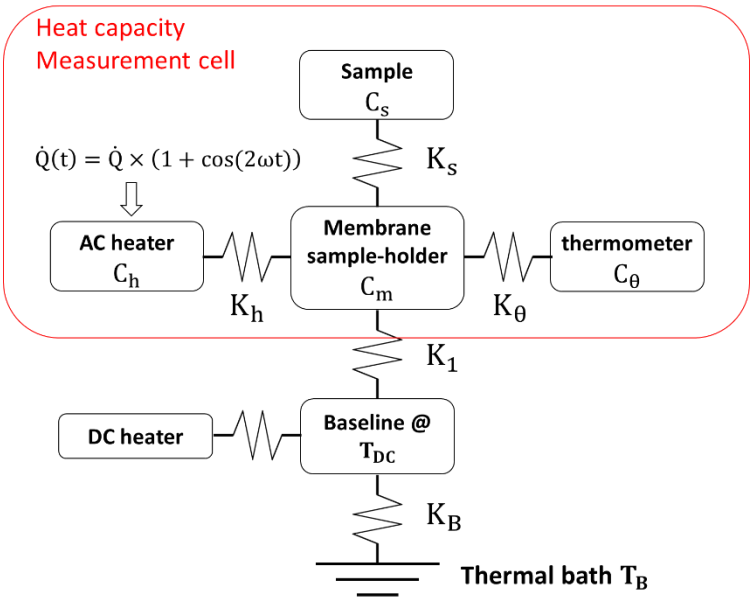

Figure 2. architecture of a typical free-standing technology cell.

The cell involves four bodies: the AC heater, the thermometer, the membrane and the sample. The temperature of the sample is controlled in two levels: a guard ring generally imposes the static temperature T_{DC}. The modulation of temperature is obtained by a AC heater coupled to the membrane. The sample is fixed on the membrane and the thermometer records the membrane's temperature.

Note that this free-standing membrane architecture creates a sub cell (sample-holder) that operates independently of the presence of a sample. The sample holder should therefore be characterized separately as it provides the oscillating cell temperature.

4. Effect of the exchange time constants to the frequency response of the cell

Under steady-state conditions, the exact expressions of the temperature are obtained by solving the system of four equations involving a first-degree differential equation for each body:

$$C\frac{dT_i}{dt} = \sum_{j \neq i} K_j(T_j - T_i) \qquad (4)$$
$$i = 1 \text{ to } 4$$
$$T_i(t) = T_i e^{J(2\omega t - \varphi_i)}$$

The calculations lead to a solution in the complex plane. The amplitude of the temperature is done by the modulus of the result since its phase shift is done by the imaginary term. The calculations are performed successively for the sample (Eq. 5) and for the sample-holder (Eq. 6), whose temperature is quantified by the thermometer.

In a development of the 1st order in $1/\omega^2$, $\omega^2$and ω^4, the approximate shape of the sample temperature shows its complex interactions with the exchange times of the bodies. Note that the tree bodies of Figure 2 (thermometer, heater and sample) play a symmetrical role with respect to the membrane. Note that the Sullivan & Seidel results are derived to Eq. 5 by setting $C_s = 0$ and $C_m = C_s$ which refers to a three bodies architecture of their cell.

The temperature of the sample-holder has the same shape as that of the sample. However, the exchange times of the sample, the thermometer and the heater to the membrane respectively change

the response of the membrane. The key factor is the thermal coupling K_h and its exchange time $\tau_{e,h}$: If the measurement periodicity τ is not matched to $\tau_{e,h}$ (i.e. $\tau/\tau_{e,h} \gg 1$), the AC power will not propagate through the membrane and the cell will be inefficient in sensing the sample. Even if the AC heat transfer is effective, there is no guarantee that the sample will be probed because its exchange time is a priori different from that of the thin film sensors. The amplitude of the sample-holder temperature oscillation could be increased simply by a mass reduction effect (A_4 terms of Eq. 6).

$$
\begin{gathered}
T_s(t) = T_{static} + \widetilde{T}_s(t) \\
T_{static} = T_{DC} + \frac{P_h + P_\theta}{K_1} \\
\widetilde{T}_s(t) = \frac{P_h}{\omega C_t} \times \frac{e^{j(2\omega t-\varphi)}}{\sqrt{(1+A_1)+\frac{1}{(\omega\tau_1)^2}+A_2\times\omega^2 + A_3 \times \omega^4}} \\
C_t = C + C_s \\
A_1 = \left(\frac{\tau_{e,s}^2}{\tau_1^2}\left(1+2\frac{K_s}{K_1}\right) + \frac{\tau_{e,\theta}^2}{\tau_1^2}\left(1+2\frac{K_\theta}{K_1}\right) + \frac{\tau_{e,h}^2}{\tau_1^2}\left(1+2\frac{K_h}{K_1}\right) \right) \\
A_2 = \begin{pmatrix} \tau_{e,\theta}^2\left(\frac{C_m+C_s+C_h}{C_t}\right) + \tau_{e,h}^2\left(\frac{C_m+C_s+C_\theta}{C_t}\right) + \tau_{e,s}^2\left(\frac{C_m+C_\theta+C_h}{C_t}\right) + \cdots \\ \frac{\tau_{e,s}^2 \times \tau_{e,\theta}^2}{\tau_1^2}\left(1 + 2\left(\frac{K_s}{K_1}+\frac{K_\theta}{K_1}\right) + 2\frac{K_s \times K_\theta}{K_1^2}\right) + \cdots \\ \frac{\tau_{e,s}^2 \times \tau_{e,h}^2}{\tau_1^2}\left(1 + 2\left(\frac{K_s}{K_1}+\frac{K_h}{K_1}\right) + 2\frac{K_s \times K_h}{K_1^2}\right) + \cdots \\ \frac{\tau_{e,\theta}^2 \times \tau_{e,h}^2}{\tau_1^2}\left(1 + 2\left(\frac{K_\theta}{K_1}+\frac{K_h}{K_1}\right) + 2\frac{K_\theta \times K_h}{K_1^2}\right) \end{pmatrix} \\
A_3 = \tau_{e,\theta}^2 \times \tau_{e,h}^2 \left(\frac{C_m + C_s}{C_t}\right)^2 + \tau_{e,\theta}^2 \times \tau_{e,s}^2 \left(\frac{C_m + C_h}{C_t}\right)^2 + \tau_{e,h}^2 \times \tau_{e,s}^2 \left(\frac{C_m + C_\theta}{C_t}\right)^2
\end{gathered}
\tag{5}
$$

Eq. 5. temperature of the sample

$$
\begin{gathered}
T(t) = T_{static} + \widetilde{T}(t) \\
\widetilde{T}(t) = \frac{P_h}{\omega C_t} \times \frac{\sqrt{1 + A_4 \times \omega^2}}{\sqrt{(1+A_1)+\frac{1}{(\omega\tau_1)^2}+A_2\times\omega^2 + A_3 \times \omega^4}} \times e^{j(2\omega t-\varphi)} \\
A_4 = \left(\tau_{e,s}^2 + \tau_{e,\theta}^2 + \tau_{e,h}^2\right)
\end{gathered}
\tag{6}
$$

Eq. 6. Temperature of the sample-holder

We now propose an analyzing of a 5 µm free-standing polymer membrane deposited on a copper disk [RIOU, 1997]. Thermometer and heater are thin-film deposited and lithographically patterned within a central area of 0.5 mm diameter. Due to the reproducibility of the technique used, the sample-holder contribution to the total heat capacity is evaluated to within 10% of accuracy and is of the order of 1 µJ/K at 100K. The device is optimized for the temperature range [40K; 160K]. The thermal drift of T_{static} is less than $1\ \mathrm{mK/h}$. The device was used for investigating the YBaCuO phase diagram with high resolution and high accuracy [4].

In most cases, the sensors are made of metals thin-film deposition techniques on the membrane, which are forwarded micro-machined by lithography. The process ensures an optimal surface thermal

conductivity $k \sim 1\ W\ cm^{-2}\ K^{-1}$ [15]. The exchange times can then be evaluated by the relation $\tau_e = \rho ct/k$. They vary linearly with the film thickness. Estimates are given in Table 1 for an YBaCuO sample with an exchange area of $\sim 0.04\ mm^2$ and a thickness of $\sim 43\ \mu m$. The sample mass is $\sim 10\ \mu g$.

	unity	thermometer (copper)	AC heater (Constantan)	YBaCuO	Membrane (Polyphenylquinoxaline)	Isotherm (Gold)
t	µm	0.4	0.15	50	5	0.9
ρ	g/cm^3	8.96	8.7	6.4	1.22	19.3
c	J/g K	0.25	0.25	0.19	0.4	0.11
κ	$W\ m^{-1}\ K^{-1}$	340	20	10	0.13	300
k	$W\ cm^{-2}\ K^{-1}$	1	1	1	-	1
τ_e	ms	0.1	0.03	6	-	0.2

Table 1. Estimates of the exchange times constant $\tau_e = \rho ct/k$ of a free-standing membrane cell. The characteristics of YBaCuO are issue of [16]. $\tau_{e,s}$ is evaluated for a tipical thickness of 50 µm. Values are indicated at 100K.

The thermal exchange times are evaluated in the heat transverse mode. By the exception of the sample, they are typically of 0.1 ms. The choice to minimize the thickness of the AC heater ensures that the heat wave propagates through the membrane over a wide excitation frequency range. The cell contains a fifth body (gold thin film of 0.6 mm diameter). It is sputtered in the center of the backside of the membrane and it serves both as an isothermal surface and to bond the sample by the gold-gold diffusion process. We do not consider its contribution to the dynamics of the heat exchanges since its exchange time is not limiting comparing to the same of the sample, nor its internal time constant due to its high thermal diffusivity.

Table 2. shows the values of thermal conductance of the cell.

	unity	designation	Value
K_1	µW/K	Thermal conductance of the cell to the baseline	13 - 14
K_h	mW/K	Thermal conductance of the AC heater to the membrane	0.5 - 1
K_θ	mW/K	Thermal conductance of the thermometer to the membrane	0.5 - 1
K_s	mW/K	thermal conductance of the sample to the membrane	0.4 - 0.8

Table 2. Estimated thermal conductance of the cell. $K_1 = dP/dT$ is derived from the $P(T)$ characteristic during a calibration sequence of the sample-holder [2]. The other thermal conductances are estimated by geometrical consideration ($K = k \times A$). Estimates for lithographed sensors are subject to variability due to the difficulty in accurately assessing their effective contact area. Values are indicated at 100K.

The addendum contributions reach $C_t \sim 1.1\ \mu J/K$ at 100K. By comparison with K_1 (Table 2), the adiabatic time constant τ_1 can be estimated to be 0.08 s. In the case of an empty cell, the condition $1/(\omega\tau_1)^2 < 0.1$ is satisfied above 6.5 Hz of excitation frequency. By adding a 10 µg of sample to the cell, the total heat capacity is increased to 3.6 µJ/K and the adiabatic time constant is $\tau_1 \sim 0.25$ s. The adiabatic

condition is then satisfied above 2 Hz. On the other hand, the ratio $m = C_s/C_t$ is about 0.7:1, which is very favorable for the measurement of its heat capacity with accuracy.

Table 3. shows the estimated contribution of each body to the heat capacity.

	unity	thermometer (copper)	AC heater (Constantan)	YBCO	Membrane (Polyphenylquinoxaline)	Isotherm (Gold)
C	µj/K	0.04	0.02	2.43	0.58 ± 0.1	0.46 ± 0.1

Table 3. Estimated heat capacities $C = \rho cAt$ of the cell. The specific heat of the membrane has been characterized previously [17]. The heat capacities are estimated by geometrical consideration. The uncertainty indicates a variability of the effective diameter between 0.5 mm (total sensor diameter) and 0.6 mm (gold isotherm diameter). Values are indicated at 100K.

In Table 4, we analyze the influence parameters A_i that govern the thermodynamic behavior of the membrane. The suffix i indicates the contribution of each term of Eq. 6.

Influence parameter	Unity	A_{i1}	A_{i2}	A_{i3}	A_{i4}	A_{i5}	A_{i6}
A_1	dimensionless	0.05	0	0	-	-	-
A_2	ms^2	0.01	0	11.6	0.03	0	0
A_3	ms^4	0	0.03	0	-	-	-
A_4	ms^2	36	0.01	0	-	-	-

Table 4. Analysis of the influencing parameters A_i that govern the thermodynamic behavior of the membrane. Each term A_{ij} is analyzed with respect to its order of appearance in Eq. 6. We have rounded their values to the second order and we do not take into account their contribution of lower order.

The analysis shows that the thermodynamic behavior of the cell is mainly dominated by the sample one together with the thermometer one. By keeping the second order influencing parameters, we rewrite the expression of the sample-holder temperature as follows:

$$
\begin{aligned}
T(t) &= T_{static} + \tilde{T}(t) \\
T_{static} &= T_{DC} + \frac{P_h + P_\theta}{K_1} \\
\left|\tilde{T}(t)\right| &= \frac{P_h}{\omega C_t} \times \frac{\sqrt{1 + A_4^* \, \omega^2}}{\sqrt{(1+A_1^*) + \frac{1}{(\omega \, \tau_1)^2} + A_2^* \, \omega^2 + A_3^* \, \omega^4}} \\
C_t &= C + C_s \\
A_1^* &= \left(\frac{\tau_{e,s}}{\tau_1}\right)^2 \times \left(1 + 2m \frac{\tau_1}{\tau_{e,s}}\right) \\
A_2^* &= \tau_{e,\theta}^2 \left(1 - \frac{C_\theta}{C_t} + m^2 \times \frac{K_1}{K_s}\left(1 + 2\left(\frac{K_s}{K_1} + \frac{K_\theta}{K_1}\right) + 2\frac{K_s \times K_\theta}{K_1^2}\right)\right) + \tau_{e,s}^2 (1-m) \\
A_3^* &= \tau_{e,\theta}^2 \times \tau_{e,s}^2 \left(1 - \frac{C_\theta}{C_t} - m\right)^2 \\
A_4 &= \left(\tau_{e,s}^2 + \tau_{e,\theta}^2\right) \\
m &= C_s/C_t
\end{aligned}
\qquad (7)
$$

5. Effect of the thermal diffusivity of the sample

The discussion in the previous subsection cannot be applied to a real system without considering the influence of the finite thermal diffusivity $D = \kappa/\rho c$ of the sample.This coefficient is suitable for modeling the directional heat transfer inside a homogeneous plate-shaped sample of thickness t being probed by periodic thermal excitation of pulsation ω.

To determine the effect of the finite diffusivity, we consider the case illustrated in Figure 3.

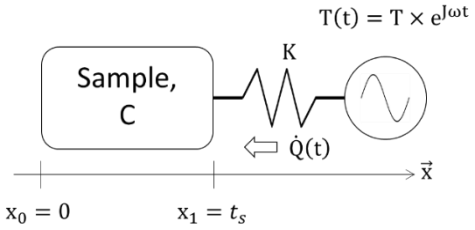

Figure 3. Effect of the thermal diffusivity on the transverse heat transfer inside homogeneous plate-shaped sample of thickness t_s. The sample is probed by periodic thermal excitation of pulsation ω through a thickness-less thermal conductance K.

The sample (thickness t, cross-sectional area A, heat capacity C) is probed by a sinusoidal excitation $T(t)$ through a thickness-less thermal conductance K. At the abscissa x_1, the sample is uniformly heated by a sinusoidal heat flux $\dot{q}_1(t) = \dot{Q}/A_s \; e^{i\omega t}$ per unit area. Let's note $T_1(t)$ its cross-sectional temperature. The other side of the sample (abscise x_0) is characterized by $\dot{q}_0(t) = 0$ by assuming no heat exchange on the outer surface of the sample. its temperature is noted $T_0(t)$.

To complete the description, we also introduce the directional penetration length $L_x = \sqrt{2D/\omega}$ and its reciprocal propagation wave vector $k_x = 1/L_x$, together with the internal time constant of the sample $\tau_{i,s} = t_s^2/(\sqrt{90} \times D)$ in the case of unidirectional heat transfer mode. $\tau_{i,s}$ is associated with the time required for the sample to reach thermal equilibrium.

The heat transfer through K is effective only if $(\omega\tau_{e,s})^2 \ll 1$ where $\tau_{e,s} = C/K$. Thus, the heat transfer regime could be studied in the steady periodic state. Such problems are easily solved by the matrix method [18]. The matrix method always be interested in two quantities: the temperature $T(x,t)$ and the surface flux $\dot{q}(x,t)$. In the case shown in Figure 3, the temperature and the heat flux at the free cross sectional area at the abscissa $x = 0$ verify the following matrix equation [18]:

$$\begin{pmatrix} T \\ \dot{q} \end{pmatrix} = \begin{pmatrix} 1 & -1/K \\ 0 & 1 \end{pmatrix} \begin{pmatrix} \mathcal{A} & \mathcal{B} \\ \mathcal{C} & \mathcal{D} \end{pmatrix} \begin{pmatrix} T_0 \\ 0 \end{pmatrix} = \begin{pmatrix} T_0 \times (A - C/K) \\ T_0 \times C \end{pmatrix}$$

$$\mathcal{A} = \cosh(k_x t_s(1+i)) \qquad \mathcal{B} = -\frac{\sinh(k_x t_s(1+i))}{\kappa_s \, k_x (1+i)}$$

$$\mathcal{C} = -\kappa_s \times k_x \, (1+i) \sinh(k_x t_s(1+i)) \qquad \mathcal{D} = \cosh(k_x t_s(1+i)) \tag{8}$$

$$T_0(t) = \frac{\dot{q}}{\mathcal{C}} = -\frac{\dot{Q}}{K_s \times \theta \sinh(\theta)} e^{i\omega t}$$

$$K_s = \frac{\kappa_s A_s}{t_s}$$

The expression of the T_0 term differs from the case study of Sullivan & Seidel. The differences lie in the architecture of their cell: the sample is directly connected to a thermal bath and it is uniformly heated on its one side and its temperature is measured on the other side [10]. In the case of free-standing thin-film membrane technology, the sample and the sample-holder form a heterogeneous bulk medium in which

the adaptation of the exchange time constants of each component to the excitation frequency is a key factor. Since the quasi-static condition $\left(\omega\tau_{e,i}\right)^2 \ll 1$ is required to ensure the heat transfer between components, the thermal conductance K coupling the sample to the membrane in doesn't play any role.

The expression of the $T_0(t)$ term of the equation 8 implements a complex constant $\mathcal{C}$ of the argument $\theta = k_x t_s(1+i)$. Under the condition that the sample dimension t_s is small with respect to the characteristic thermal length L_x (i.e., $k_x t_s < 1$), $|\theta|$ must be of first order: the expansion of the term $\theta\sinh(\theta)$ then does not need to be done above the third order.

The approximation of the complex amplitude of $T_0(t)$ and its modulus is then expressed as:

$$T_0 \approx \frac{\dot{Q}}{K_s} \times \frac{1}{\theta\left(\theta + \frac{\theta^3}{3!} + o(\theta^4)\right)}$$
$$|T_0| \approx \frac{\dot{Q}}{\omega C_s \sqrt{1 + \frac{5}{2}\left(\omega\tau_{i,s}\right)^2 + o(\omega^4)}} \qquad (9)$$

The result shows that the oscillating temperature of the sample is inversely proportional to its heat capacity under the quasi-static condition that $(2.5 \times \omega\tau_{i,s})^2 \ll 1$. Note that this condition is more restrictive in the case of free-standing membrane technology than in the cell architecture of Sullivan & Seidel which states ${\omega\tau_{i,s}}^2 \ll 1$. Respecting a fourth order limit development, the expression of the sample-holder temperature must be completed by the additive term $(2.5 \times \omega\tau_{i,s})^2$ in Equation 7.

6. Effect of the thermal diffusivity of the membrane

The membrane is the site of complex heat exchanges between the sensors and the sample across the membrane. Depending on the thermal conductivity of the membrane, its thickness and the cell architecture, the internal time constant $\tau_{i,m}$ can vary considerably, depending on whether the heat transfer modes are transverse or longitudinal.

In a previous work [2], we analyzed the frequency behavior of a free-standing membrane cell implementing a 5µm thick membrane of polyphenyl-quinoxaline ($\kappa_m \approx 0.13\ \mathrm{WK^{-1}m^{-1}}$ at 100K) equipped with two YBaCuO samples of different sizes (Figures 4 & 5). The result is showed in Table 5.

Sample	$\tau_{i,s}$	$\tau_{e,s}$	m	$\tau_{i,m}$
Unity	ms	ms	-	ms
YBCO #3	1.5	5.2	0.68	4.2
UBC #2	0.7	3.5	0.86	1.6

Table 5. Internal time constant of the membrane deduced from the frequency analysis of the cell [2].

Table 5 highlights the critical role of the membrane, as its internal time constant determines the dynamic behavior of the cell. A large sample promotes transversal heat exchange due to its proximity to the AC heater. This results in a decrease in the internal time constant and increases the accuracy of the heat capacity of a few µg samples. As mentioned above, the lithographic AC heater and the thermometer

play a symmetrical role: An optimal configuration is then to place the sample symmetrically between the heater and the thermometer sensors.

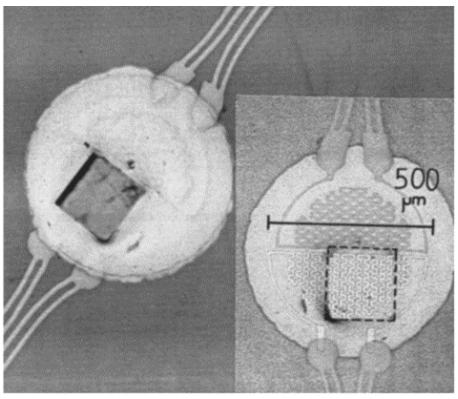

Figure 4. Photograph of YBaCuO#3 sample (11 µg, $t_s \approx 43\mu m$, $A_s \approx 0.04\ mm^2$). Inset: Top meander: AC heater, bottom meander: thermometer. The crystal mark is shown as a dotted line. The sample is bonded below the thermometer: this promotes longitudinal heat exchange through the membrane and provides long internal time constant

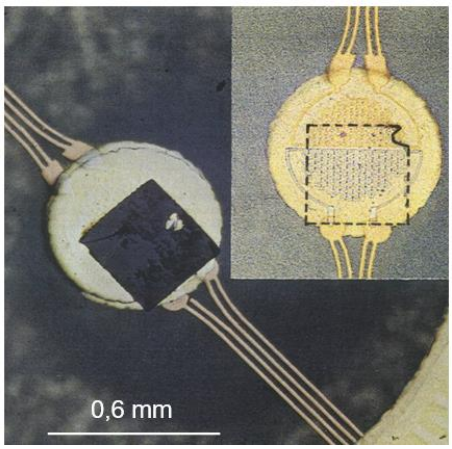

Figure 5. Photograph of UBC#2 sample (33 µg, $t_s \approx 29\mu m$, $A_s \approx 0.18\ mm^2$). Inset: Top meander: AC heater, bottom meander: thermometer. The crystal mark is shown as a dotted line. The sample is bonded below the thermometer and extends to the AC heater due to its larger size. This promotes transversal heat exchange through the membrane and provides shorter internal time constants

In the free-standing thin film membrane architecture, the sample-holder behaves like the sample. Respecting a fourth order limit development, the expression of the sample-holder temperature must be completed by the additive term $(2.5 \times \omega\tau_{i,m})^2$ in Equation 7.

7. Effect of the thermal diffusivity of the electrical contacts

Regardless of the cell architecture, some of the heat diffuses along the electrical contacts. The heat leaks affect the amplitude of the oscillating temperature of the cell. To quantify the effect of the heat leaks, we consider the situation illustrated in Figure 6.

The steady-state heat transfer is modeled in the matrix method (Figure 7). The composite medium is characterized by its specific heat c_c, a thermal conductivity κ_c and a specific mass ρ_c. Let T and $\dot{q}$ be the temperature and the surface heat flux at the cross sectional area specified by the abscissa x_0. The others

(T_∞ and $\dot{q}_\infty$) are given by the free abscissa x_∞. The heat transfer is assumed to be uniform over the composite area A_c and its free thickness is $t_c = x_\infty - x_1$. In the absence of convective or radiative exchange on the outer surface of the composite medium, heat flow is maintained through each cross-section then $\dot{q}_\infty = \dot{q}$.

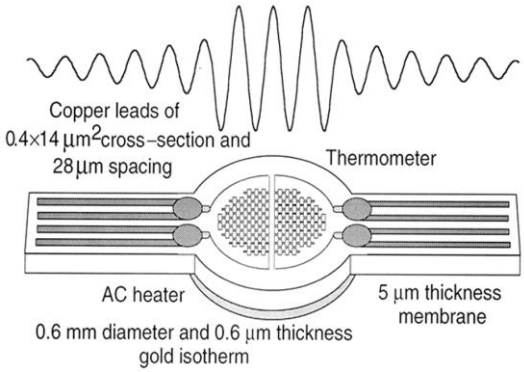

Figure 6. Freestanding thin-film membrane technology. The electrical wires diffuse a part of the AC heat. They form with the membrane a composite medium of a thermal diffusivity D_c. Assuming of a unidirectional propagation, the thermal oscillations are damped as $\exp(-k_x(\omega) \times x)$.

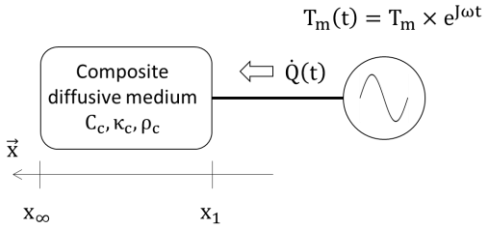

Figure 7. 1D Model of the steady-state heat transfer in the composite medium treated by the matrix method. The abscissa x_1 refers to the cell boundary.

The heat transfer inside the composite medium is governed by the matrix equation:

$$\begin{pmatrix} T_m \\ \dot{q} \end{pmatrix} = \begin{pmatrix} \mathcal{A} & \mathcal{B} \\ \mathcal{C} & \mathcal{D} \end{pmatrix} \begin{pmatrix} T_\infty \\ \dot{q} \end{pmatrix}$$

$$T_m(x_1, t) = \frac{1 - \cosh(\theta)}{\kappa_c \, k_x (1 + i) \times \sinh(\theta)} \, \dot{q} \, e^{\,i\omega t} \qquad (10)$$

$$\theta = k_x \, x \, (1 + i)$$

$$k_x \, x = (\omega x^2 / 2D)^{0.5}$$

Equation 10 models the effect of the heat diffusion on the temperature of the membrane at the abscissa x_1. The θ argument is function of the variable $X = k_x \, x$ which is spatially, thermally and frequency dependent. On the other hand, Euler's relations can be used to expand the hyperbolic functions as a function of X (Note that $\cosh(iX) = \cos(X)$ and $\sinh(iX) = i \times \sin(X)$). The modulus of the $T_m(t)$ term is :

$$|T_m(x_1)| = \frac{\dot{Q}}{\sqrt{2} \, K_c \times f(X)}$$

$$K_c = \kappa_c A_c / x \qquad (11)$$

$$f(X) = X \, \frac{\sqrt{(\sinh^2(X) + \sin^2(X))}}{\cosh(X) - \cos(X)}$$

$$X = k_x \, x = (\omega x^2 / 2D)^{0.5}$$

K_c represents the thermal conductance of the semi-infinite composite medium of thickness x. The amplitude of X varies as $\sqrt{(90^{0.5}/2) \times \omega\tau_{i,c}}$ where $\tau_{i,c} = x^2/\sqrt{90}D$. Figure 8 shows the representation of f (X):

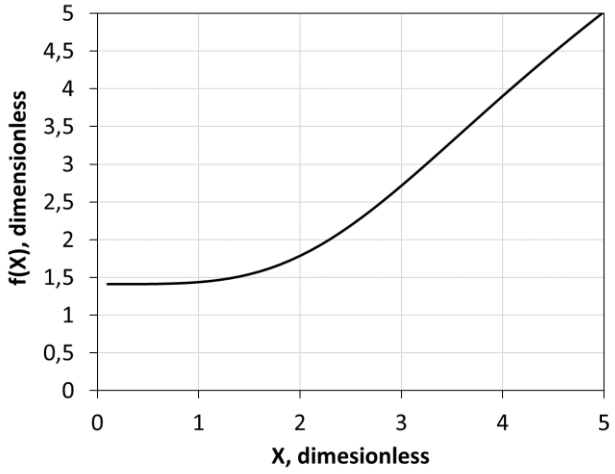

Figure 8. Effect of the semi-infinite composite medium on the amplitude of the oscillating membrane temperature $|T_m(x_1)|$ versus $X = (\omega\, x^2/2D_c)^{0.5}$. For $X \leq 1$, $f(X) = \sqrt{2}$.

The function f (X) exhibits the limiting form: below $X \leq 1$, f (X) is constant regardless of the values of the triplet (ω, D_c, x). Then $|T_m(x_1)| \approx \dot{Q}/2K_c$. This means that for a composite medium, when the excitation frequency is sufficiently low, the heat diffusion along the electrical leads will gives a constant contribution to the specific heat proportional to the thickness x of the probed composite. Its amplitude is done by the thermal conductance $K_c = \kappa_c A_c/x$. Since the probed thickness x is proportional to the thermal length penetration $L_{x,c}(\omega)$ (i.e. $x = \alpha \times \sqrt{2D_{x,c}/\omega}$), the denominator of $|T_m(x_1)|$ of Equation 11 varies as $\sqrt{\omega}$ and its associated amplitude is $\sqrt{C_c K_c/2\alpha^2}$ in $J\,K^{-1}\,Hz^{0.5}$ unity. The composite medium contributes then to the heat capacity of the cell as:

$$
\begin{gathered}
|T_m(x_1)| = \frac{\dot{Q}}{C_\omega\, \omega} \\
C_\omega = \sqrt{\frac{C_c K_c}{2\alpha^2}} \times \frac{1}{\sqrt{\omega}} \\
K_c = \kappa_c A_c/x \\
C_c = \rho_c c_c A_c x \\
\alpha = x/L_c\,(\omega) \\
X \leq 1
\end{gathered}
\qquad (12)
$$

Above $X > 3$, f (X) is proportional to X (Figure 8). The denominator of $|T_m(x_1)|$ of Equation 11 also varies as $\sqrt{\omega}$ and its associated amplitude is $\sqrt{C_c K_c}$ in $J\,K^{-1}\,Hz^{0.5}$ unity. The composite medium then contributes to the cell heat capacity as:

$$
\begin{gathered}
|T_m(x_1)| = \frac{\dot{Q}}{C_\omega\, \omega} \\
C_\omega = \sqrt{C_c K_c} \times \frac{1}{\sqrt{\omega}} \\
X \geq 3
\end{gathered}
\qquad (13)
$$

Note that the $C_c \times K_c$ term is temperature dependent only. Regardless of the limiting forms of $f(X)$, one can predict a heat capacity contribution C_ω of the electrical leads with a frequency dependence $\omega^{-0.5}$ [6]. In practice, the difficulty in quantifying its contribution lies in the values of the triplet (ρ_c, κ_c, c_c) and their temperature dependences.

8. Temperature of the sample-holder

Taking into account Sections 5 and 7 and keeping only the terms up to order ω^4, we rewrite the oscillating term of the sample-holder temperature as:

$$\left|\tilde{T}(t)\right| = \frac{\dot{Q}}{\omega} \times \frac{\sqrt{1 + A_4^* \, \omega^2}}{(C_\omega \times \omega^{-0.5}) + C \times \sqrt{(1+A_1^*) + \frac{1}{(\omega \, \tau_1)^2} + A_2^* \, \omega^2 + A_3^* \, \omega^4}}$$

$$A_1^* = \left(\frac{\tau_{e,s}}{\tau_1}\right)^2 \times \left(1+2m\frac{\tau_1}{\tau_{e,s}}\right) + \frac{5}{2}\,\frac{\tau_{i,s}^2 + \tau_{i,m}^2}{\tau_1^2}$$

$$A_2^* = \tau_{e,\theta}^2 \left(1 - \frac{C_\theta}{C_t} + m^2 \times \frac{K_1}{K_s}\left(1 + 2\left(\frac{K_s}{K_1} + \frac{K_\theta}{K_1}\right) + 2\,\frac{K_s \times K_\theta}{K_1^2}\right)\right) + \tau_{e,s}^2(1-m) + \frac{5}{2}\left(\tau_{i,s}^2 + \tau_{i,m}^2\right) \qquad (14)$$

$$A_3^* = A_2^* \times \frac{5}{2}\left(\tau_{i,s}^2 + \tau_{i,m}^2\right) + \tau_{e,\theta}^2 \times \tau_{e,s}^2 \left(1 - \frac{C_\theta}{C_t} - m\right)^2$$

$$A_4^* = \left(\tau_{e,s}^2 + \tau_{e,\theta}^2\right)$$

$$m = C_s / C_t$$

As we have described the nature of the addenda, we are able to accurately evaluate their contributions. This makes it possible to measure samples whose heat capacity C_s is of the order of $C + C_\omega$ terms, or less with a good accuracy. These performances can be reached in the majority of the existing micro-calorimeters using an AC modulation. The calorimeter developed by Sullivan & Seidel does not take into account the diffusive contribution C_ω from the total heat capacity $C + C_s$. Therefore, the authors preferred to measure sufficiently massive samples such as $C_s \gg (C_\omega, C)$ in order to improve the accuracy of the measurement. On the other hand, we pointed out that the frequency behavior of the free-standing thin film membrane architecture is still different from that of Sullivan & Seidel.

The key point is to define the frequency range in which the sample is fully probed. Due to the large number of parameters that affect the frequency response of the sample-holder temperature, we resort to its transfer function:

$$TF(\omega) = \frac{\left|\tilde{T}\right| \times C\,\omega}{\dot{Q}} \qquad (15)$$

The TF should be as close to 1 as possible, which means that the conditions of quasi-staticity and adiabaticity are met. The accuracy of the heat capacity measurement is then optimal since the error function $\mathrm{erf}(\omega) = 1 - TF(\omega)$ (Eq. 3). The choice of the frequency is thus possible if we closely analyze the transfer function of the sample-holder over a large frequency range. The concept of addenda of measurement is here considered as a precaution: one should consider a bulk and a diffusive contribution together following the form of Eq. 14. A fitting process of the TF experimental data will then lead to the set of the influence parameters A_i^* and to the C_ω term.

9. Solve the problem of the heat capacity of the wires

As already mentioned, the C_ω term seems to be constant in the range [3Hz; 11Hz]. Its value is useful to evaluate the fraction α of the thermal penetration length along the copper wires. α allows to quantify the effective thickness x of the composite medium probed by the oscillating thermal power (Eq. 12).

A portion of the membrane carries eight copper wires which serve for electrical connection (Figure 6). A cross-sectional drawing of the composite is shown in Figure 9.

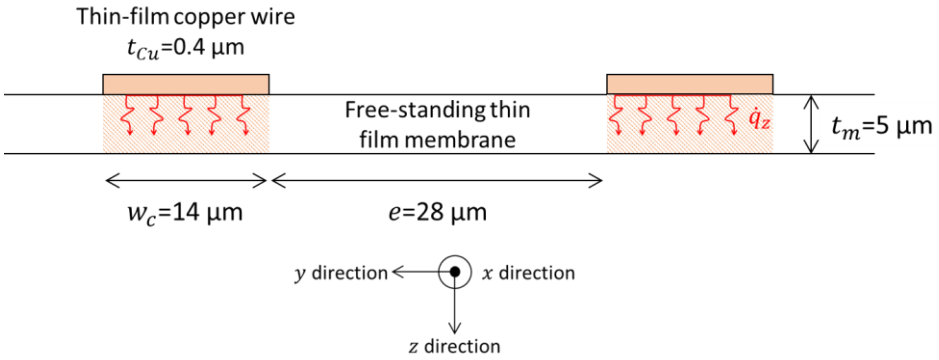

Figure 9. Cross-sectional drawing of the composite. The principal directions of the heat transfer are indicated

Thermal power propagation is effective in the x-direction, while it is continuously dissipated in the z-direction. Thanks to the low thermal conductivity of the membrane, we neglect the heat propagation in the y-direction, then each copper wire behaves independently and the study can be done on a single composite. Its dimensions are then w_c (width) and $t = t_{Cu} + t_c$ (thickness) with an longitudinal exchange area $w_c \times x$.

The thermal characteristics of the composite medium are its heat capacity, that comes mainly from the membrane and its thermal conductivity provided by the cooper leads. In this context, we propose to characterize the composite by its following thermal properties showed in Table 6:

Designation	Formulae	Unity
Linear heat capacity	$C_c = (\rho c)_m \times w_c t_m$	$J\,K^{-1}m^{-1}$
Thermal conductivity	$\kappa_c = \kappa_{Cu} \times \frac{t_{Cu}}{t}$	$WK^{-1}m^{-1}$
Linear thermal conductance	$K_c = \kappa_c \times w_c\, t_m$	$WK^{-1}m$
Thermal diffusivity	$D_c = \frac{\kappa_c}{(\rho c)_m \frac{t_m}{t} + (\rho c)_{Cu} \frac{t_{Cu}}{t}}$	$m^2\,s^{-1}$

Table 6. Thermal characteristics of the composite along the x-direction. $t = t_{Cu} + t_c$ is the total thickness of the medium.

Properties are defined in proportion to the volume of each component. Since the surface area is common, thermal properties are only thickness dependent.

Using the thermal values at 100K from the Table 1, one can successively quantify the linear heat capacity $C_c \approx 34\ \mu J\,K^{-1}m^{-1}$, the thermal conductivity $\kappa_c \approx 25\ WK^{-1}m^{-1}$, the linear thermal

conductance $K_c \approx 0{,}002\ \mu W K^{-1} m$ and the thermal diffusivity $D_c \approx 3\ 10^{-6}\ m^2 s^{-1}$. We then derive the value of $\alpha = \sqrt{C_c\ K_c/(2C_\omega^2)} \approx 5{,}3\%$.

For the thermal excitation frequency of the to 3Hz, the thermal penetration length is $L_c(\omega) \approx 0{,}55\ mm$ and the effective length of the probed composite in the x-direction is $x \approx 30\ \mu m$. These estimates are valid in the range [3Hz; 11Hz] where the C_ω term is assumed to be constant. It is probably still valid above 3Hz as X tends to 0 (Eq. 12). Figure 10 shows the evolution of x versus the frequency of the thermal excitation in the range [0Hz; 11Hz].

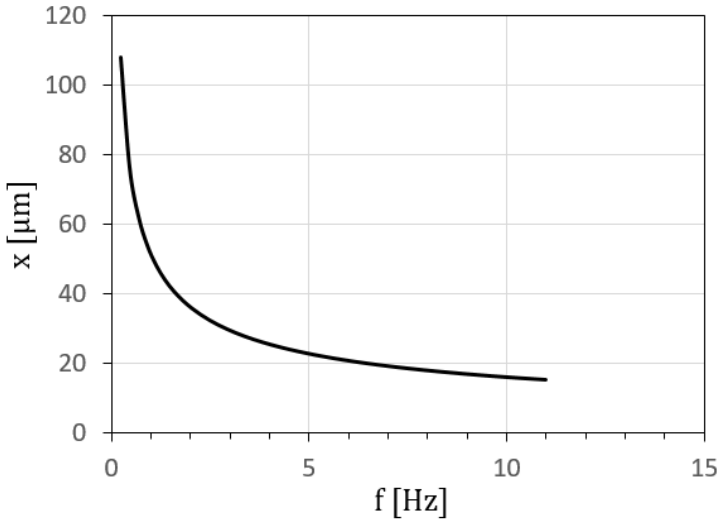

Figure 10. Effective length versus the frequency of the composite ($D_c \approx 3\ 10^{-6}\ m^2/s$ at 100K)

As the frequency decreases, x increases up to sub-millimeter values. Note that this is a long-range effect. The amplitude of x depends mainly on the directional thermal diffusivity as $D_c^{0.5}$: this behavior will be enhanced by the use of full metallic wires (as thermocouple), for which the thermal diffusivity is of the order of $10^{-5} - 10^{-4}\ m^2/s$, and the effective thermal length can then reach millimeter values [6].

10. Transfer function of the sample-holder in the case of $C \approx C_\omega(\omega)$

In the case of small samples, it is essential to separate the diffusive contribution from the sample-holder one of the transfer function. It serves to correctly fix the frequency of the thermal excitation.

The method is carried out on a free-standing thin-film membrane architecture. its thermal characteristics are shown in Table 7a.

	unity	value
C_{cell}	µJ/K	1.0
C_ω	µj $K^{-1}Hz^{0.5}$	3.4
τ_1	ms	80
$\tau_{i,m}$	ms	4.7

Table 7a. thermal characteristics of the cell at 100K [RIOU]

The diffusive contribution $C_\omega(\omega) = C_\omega \times \omega^{-0.5}$ in the unit µJ/K has already been experimentally quantified at 3Hz and 11Hz. The value of the C_ω term in the unit $J\ K^{-1}\ Hz^{0.5}$ can be deduced to be 3.38 and 3.40, respectively: The C_ω term seems to be constant in the range [3Hz; 11Hz]. The internal time

constant of the membrane is experimentally quantified by analyzing the transfer function of a cell equipped with a sample of YBaCuO #3 (Figure 4). Due to its small size, it promotes longitudinal heat exchange and we found $\tau_{i,m} = 5.2$ ms. Table 6b shows the values of the influence parameters A_i. Note that the quadruplet $(C_s, K_S, \tau_{e,s}, \tau_{i,s})$ is zero in the case of an empty cell, which means that $A_1 = A_3 = 0$.

	unity	value
A_1^*	dimensionless	$9.3\ 10^{-3}$
A_2^*	s^2	$5.5\ 10^{-5}$
A_3^*	s^4	$3.0\ 10^{-9}$
A_4^*	s^2	$8.0\ 10^{-9}$

Table 7b. influence parameters A_i of the cell at 100K

The transfer function $|\tilde{T}| \times C\omega/\dot{Q}$ of the cell is presented in Figure 11.

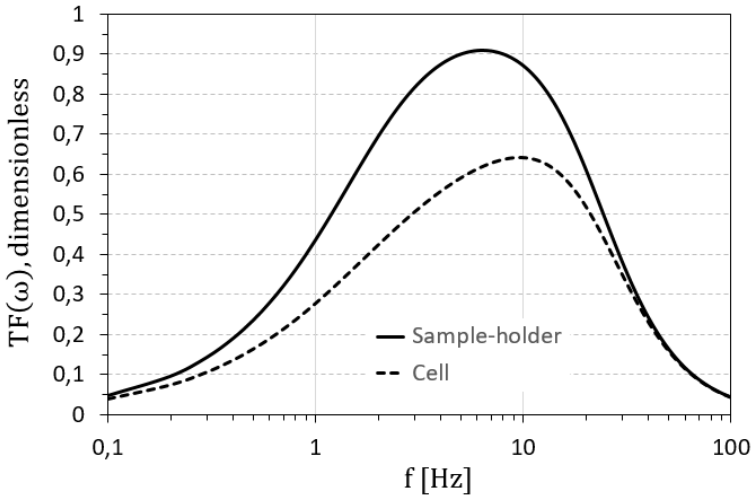

Figure 11. Transfer function $|\tilde{T}| \times C\omega/\dot{Q}$ of the cell (solid line: sample-holder, dashed line: empty Cell including the diffusive contribution of the wires

Figure 11 shows that the sample-holder behaves as expected from the Sullivan and Seidel model. The transfer function shows a standard band pass filter with two characteristic cut-off frequencies corresponding to τ_1 and τ_2 of equation 2. The frequency of the excitation power must be chosen within this limit according to the set of influencing parameters inherent to the sample-holder. In the range $[5\text{Hz};\ 8\text{Hz}]$, the transfer function shows a plateau close to 1, which means that the conditions of quasi-staticity and adiabaticity are fulfilled and the accuracy of the heat capacity measurement is optimal ($\text{erf}\,(\omega) < 10\%$). The main source of error comes from the internal time constant of the membrane which increase the A_1^* term (Tables 7).

With respect to the cell, the diffusive contribution of the electrical connections significantly blurs the analysis of its transfer function. At first sight, a narrow plateau is observed in the range $[8\text{Hz};\ 10\text{Hz}]$, resulting from the competition between the decreasing contribution of the diffusive medium $C(\omega) \sim \omega^{-0.5}$ (Eq. 12, 13), and the increasing influence of the parameters A_2^* and A_3^* which are proportional to ω and ω^2 respectively. They reflect the non-quasistatic situation. By a simple power law effect, the plateau is systematically pushed back towards the high frequencies. As a consequence, the sample is partially probed and the $\text{erf}\,(\omega)$ could be higher than 15% if we do not take into account the effect of the diffusive contribution of the wires.

https://doi.org/10.1016/j.spmi.2003.11.006

11. Transfer function of the cell in the case of $C \approx C_s > C_\omega(\omega)$

In Figure 12, we compare the transfer function of the empty sample-holder with those loaded with the samples YBaCuO#3 (11µg) and UBC#2 (33µg).

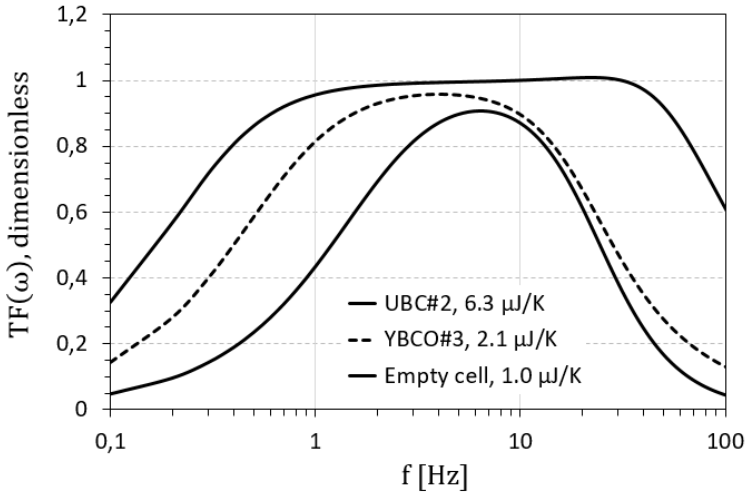

Figure 12. Transfer function of the sample-holder

Table 8 summarizes the most important facts about heat capacity measurements.

	mass	Filling factor	C	t	τ_1	$\tau_{i,m}$	$\tau_{i,s}$	erf(ω)	frequency range
	µg	-	µJ/K	µm	ms	ms	ms	%	Hz
Empty cell	-	-	1	-	77	4,7	-	10	[5Hz; 8Hz]
YBaCuO#3	11	0,67	3,1	43	232	4,7	1,5	4	[2,7Hz; 5,9Hz]
UBC#2	33	0,86	7,4	29	547	1,6	0,7	1	[2,9Hz; 34,5Hz]

Table 8.

The cell is suitable for measuring the heat capacity of samples as small as a few micrograms with an accuracy in the range of 1% to 5%. The accuracy is limited by the internal time constant of the membrane.

For the YBCO#3 sample, the decision was made to place it under the thermometer (Figure 4). This choice turns out to be a mistake because it combines a high thickness of the sample in the direction of heat transfer with a high internal relaxation time of the membrane. As a result, the measurement uncertainty is high.

For sample UBC#3, the uncertainty is reduced because the internal relaxation time of the membrane is minimized (the sample straddles the thermometer and the heater, Figure 5) and its thickness is small.

In order to optimize the heat capacity measurement ($\mathrm{erf} < 1\%$), it is then necessary to respect some precautions: first, the exchange time of the sample by increasing its thermal conductivity $K_s = k \times A_s$. For this, it is necessary to measure the sample according to its larger surface and/or to improve the thermal coupling k. It is necessary to check that the geometric A_s/t_s term remains large enough, which forces to measure the sample according to its smaller dimension [10]; secondly, The bulk sample should

be thermally coupled at the center of the cell, as this minimizes the internal time constant $\tau_{i,m}$ of the membrane [2] and thirdly, the ratio $t_s/L(3Hz)$ should be less than 0.05, depending of the thermal diffusivity D of the sample. This condition appears stricter than that already met in the literature [19].

12. conclusions

The AC modulation calorimetry today is usually used in the experiments which require a high resolution of measurement. One has to be careful of the choice of frequency which determines the accuracy of measurement.

We develop a free-standing thin film membrane technic to measure the heat capacity of bulk samples.

This technique cannot be applied without some basic precautions. We state limitations, primarily of diffusive origin. Within this framework, we proposed a formalism which makes it possible to quantify these limitations and to improve the accuracy of measurement:

- It is essential to reduce the exchange time constants of the sensing elements, particularly the heater, thermometer and sample. This can be achieved by thin film deposition techniques and gold-gold sample bonding,
- The sample must be adhered to the center of the cell to minimize the internal time constant of the membrane $\tau_{i,m}$,
- The sample's transversal thickness should be as lower as possible, in order to minimize its internal time constant $\tau_{i,s}$. the ratio $t_s/L(3Hz)$ should be less than 0.05, depending of the thermal diffusivity D of the sample.

Acknowledgements

Many thanks to Prema Menezes for reviewing the English version of this manuscript

References

[1] Yaakov Kraftmakher (2002). Modulation calorimetry and related techniques. Physics Reports, volume 356, Issues 1–2, Pages 1-117. https://doi.org/10.1016/S0370-1573(01)00031-X.

[2] O. Riou; P. Gandit; M. Charalambous; J. Chaussy (1997). A very sensitive microcalorimetry technique for measuring specific heat of μg single crystals. Review of Scientific Instruments 68, 1501–1509. https://doi.org/10.1063/1.1147938

[3] J. Chaussy, P. Gandit, J.L. Bret, F. Terki (1992). A very sensitive technique for measuring the temperature derivative of electrical resistance between 4 and 300 K, Review of Scientific Instruments 63, 3953–3958. https://doi.org/10.1063/1.1143244

[4] M. Charalambous, 0. Riou, P. Gandit, B. Billon, P. Lejay, J. Chaussy, W.N. Hardy, D.A. Bonn, R. Liang (1999). Asymmetry of critical exponents in YBaCuO. Physical Review Letters 83 (10) 2042. https://doi.org/10.1103/PhysRevLett.83.2042

[5] D.W. Denlinger, E.N. Abarra, K. Allen, P.W. Rooney, M.T. Messer, S.K. Watson, F. Hellman (1994). Thin film microcalorimeter for heat capacity measurements from 1.5 to 800 K. Review of Scientific Instruments 65, 946–959. https://doi.org/10.1063/1.1144925

[6] R.L. Greene, C.N. King, R. Zubeck (1972). Specific heat of granular aluminium film. Physical Review B 6, 3297. https://doi.org/10.1103/PhysRevB.6.3297

[7] L.R. Bachmann, F.J. Disalvo, T.H. Geballe, R.L. Grenne, R.E. Howard, C.N. King (1972). Heat capacity measurements on small samples at low temperature. Review of Scientific Instruments 43, 205-214. https://doi.org/10.1063/1.1685596

[8] T. Suzuki, T. Tsuboi, H. Takaki (1982). AC temperature calorimetry for thin films at low temperatures. Japanese Journal of Applied Physics 21 (2), https://doi.org/368. 10.1143/JJAP.21.368

[9] A.A. Minakov (1997). Low-temperature AC microcalorimetry: possibilities and limitations. Thermochimica Acta volume 304-305, pp 165-170. https://doi.org/10.1016/S0040-6031(97)00125-1

[10] P.F. Sullivan, G. Seidel (1968). Steady state ac-temperature calorimetry. Physical Review 173 (3) (1968) 679. https://doi.org/10.1103/PhysRev.173.679

[11] H.J. Fecht, W.L. Johnson (1991). A conceptual approach for non-contact calorimetry in space. Review of Scientific Instruments 62, 1299–1303. https://doi.org/10.1063/1.1142488

[12] I.V. Velichkov (1992). On the problem of thermal link resistances in ac calorimetry. Cryogenics 32 (3), 285-290. https://doi.org/10.1016/0011-2275(92)90366-I

[13] E. Gmelin (1997). Classical temperature modulated calorimetry: a review. Thermochimica Acta, volumes 304–305, 1-26. https://doi.org/10.1016/S0040-6031(97)00126-3

[14] F. Fominaya, T. Fournier, P. Gandit, J. Chaussy (1997). Nano-calorimeter for high resolution measurements of low temperature heat capacities of thin films and single crystals. Review of Scientific Instruments 68, 4191–4195. https://doi.org/10.1063/1.1148366

[15] R. Salmi (1993), Thèse de doctorat de l'Université Joseph Fourier, Grenoble. Dispositif de mesure de la chaleur spécifique de petits échantillons : application à l'$YBa_2Cu_3O_{7-\delta}$.

[16] Gold, Z.; Gagnon, R.; Ellman, B.; Taillefer, L.; Behnia, K. (1994). Anisotropic thermal conductivity of $YBa_2Cu_3O_{7-\delta}$. Physica. C: Superconductivity, Vol.235-240 (2), 1485-1486. https://doi.org/10.1016/0921-4534(94)91967-4

[17] Roberto Calemczuk (1995). He graciously measured the specific heat of PPQ samples between 40 K and 200 K. Affiliation: DRFMC-SPSMS, CEA-Grenoble, France (unpublished)

[18] H. S. Carslaw and J. C. Jaeger (1959). Conduction of heat in Solids. Oxford University Press, London, 1959, 2nd edition

[19] I. Hatta, A.A. Minakov (1999). Some remarks on heat capacity measurements by temperature-modulated calorimetry. Thermochimica Acta, volume 330, Issues 1–2, Pages 39-44. https://doi.org/10.1016/S0040-6031(99)00038-6

collaborative contribution